A Dynamical Model for the Vertical Vestibuloocular Reflex and Optokinetic Response in Primate

Yutaka Hirata[1], Ichiro Takeuchi[1], Stephen M. Highstein[2]

[1] *Dept. Electronic Engineering, Chubu University College of Engineering,*
[2] *Dept. Otolaryngology, Washington University School of Medicine*

ABSTRACT The vestibuloocular reflex (VOR) in concert with the optokinetic response (OKR) stabilizes vision during head motion. The VOR system characteristics are both compensatory and adaptively self-calibrated. A model was constructed to aid in the understanding of the roles of the cerebellum and other neuronal sites in the performance and adaptation of the vertical VOR. The model structure was based upon the known neuroanatomy, and model parameters were estimated using experimental data. The model can reproduce and predict eye movements and cerebellar Purkinje cell firing patterns during VOR, OKR, and various visual-vestibular mismatch paradigms.

INTRODUCTION

The vestibuloocular reflex (VOR) in concert with the optokinetic response (OKR) stabilizes vision during head motion. The VOR produces compensatory eye movements under adaptive control that result in a VOR gain (eye velocity / head velocity) of 1 in the light; changes in VOR-OKR system characteristics are compensatory and self-calibrating, thus changes in VOR characteristics caused by aging, injury, or visual-vestibular mismatch are adjusted to achieve compensatory eye movements. The cerebellar flocculus (FL) is necessary for VOR adaptation since its removal or inactivation precludes further changes in gain [5][10], yet the FL role in VOR adaptation has long been controversial [3][6]. FL neuronal circuitry is characterized by multimodal sensory-motor transformations involving multiple feedback loops making causality ambiguous. The complexity of this circuitry has been problematic in assigning a role to FL in the process of adaptation and performance of the VOR. The system identification approach combines electrophysiological experiments and mathematical modeling and might provide way to overcome the difficulty. Presently we built a model for the monkey vertical VOR/OKR based upon its well understood anatomy and physiology. The model is extended from our previous multiple linear regression model that was built to describe only a single frequency [2].

The present model consists of 6 subsystems each of which represents the signal processing of a sensory modality or the generation of motor and pre-motor commands in the cerebellum or in non-cerebellar structures. Characteristics of each subsystem were identified by fitting model output to experimental data with rich information in terms of frequency and amplitude, and the validity of the model was checked by predicting various experimental data that were not used for the model identification. It was shown that the model can reproduce or predict eye movements and FL Purkinje cell firing patterns during VOR, OKR, and visual-vestibular mismatch paradigms over a wide frequency range as well as those after lesion and inactivation of the FL.

METHODS

Model structure

Figure 1A illustrates the neuroanatomy of the vertical VOR/OKR in primate. In order to evaluate the possible roles of the cerebellum in VOR/OKR control and adaptation, we divided the circuit into pathways that include the cerebellum and ones that do not. Six subsystems form the model as illustrated in Figure 1B: $G^{vestib}_{preFL\&FL}(s)$, $G^{visual}_{preFL\&FL}(s)$, and $G^{ecopy}_{preFL\&FL}(s)$ describe the characteristics of pre-FL and FL pathways that process vestibular, visual and efference copy signals, respectively and convert each signal into the output of the FL Purkinje cell activity. $G_{postFL}(s)$ describes the characteristics of the post-FL pathway that converts FL Purkinje cell activity into a component of the eye movement command. $G^{vestib}_{nonFL}(s)$ and $G^{visual}_{nonFL}(s)$ describe the characteristics of the non-FL pathways that process vestibular and visual signals, respectively and convert these sensory signals into a component of the eye movement command. Neuronal circuitry that is included in $G^{visual}_{nonFL}(s)$ is not illustrated in Figure 1A due to the lack of anatomical evidence, but it is apparent that such a pathway exists because lesion of the FL does not completely diminish eye movement in response to visual stimuli [10]. System equations of the model are described as follows:

$$F(s)=H(s)G^{vestib}_{preFL\&FL}(s)+R(s)G^{visual}_{preFL\&FL}(s)+X(s)G^{ecopy}_{preFL\&FL}(s)$$

$$X(s) = F(s)G_{postFL}(s) + H(s)G^{vestib}_{nonFL}(s)+R(s)G^{visual}_{nonFL}(s)$$

where $F(s)$, $H(s)$, $R(s)$, and $X(s)$ denote the Laplace transform of FL Purkinje cell firing rate, head position, retinal slip position, and eye position, respectively while s is the Laplace operator. Each subsystem is described as the following transfer function that was determined based on known physiological evidence:

$$G^{vestib}_{preFL\&FL}(s) = (a_h s^2 + b_h s + g_h)\, e^{-p_h s} \quad (1)$$

$$G^{visual}_{preFL\&FL}(s) = (a_r s^2 + b_r s + g_r)\, e^{-p_r s} \quad (2)$$

$$G^{ecopy}_{preFL\&FL}(s) = (a_e s^2 + b_e s + g_e)\, e^{-p_e s} \quad (3)$$

$$G_{postFL}(s) = e^{-t_x s} / (a_x s^2 + b_x s + c_x) \quad (4)$$

$$G^{vestib}_{nonFL}(s) = (a_h s^2 + b_h s + c_h)\, e^{-t_h s} / (u_h s^2 + v_h s) \quad (5)$$

$$G^{visual}_{nonFL}(s) = (a_r s^2 + b_r s + c_r)\, e^{-t_r s} / (u_r s^2 + v_r s) \quad (6)$$

where a_h, b_h and g_h denote head acceleration, velocity and position sensitivity of the Purkinje cell, respectively while p_h denotes the latency of Purkinje cell firing in response to head motion. a_r, b_r, and g_r denote retinal slip acceleration, velocity and position sensitivity of Purkinje cell, respectively while p_r denotes the latency of Purkinje cell firing in response to retinal slip. Higher order terms relating to retinal slip were not included because it has been shown that retinal slip jerk does not contribute to Purkinje cell firing [4][9]. a_e, b_e, and g_e denote eye acceleration, velocity and position sensitivity of the Purkinje cell while p_e denotes the latency of Purkinje cell firing in response to eye movement. Higher order terms relating to eye movements were not included because it has been shown that eye jerk does not contribute to Purkinje cell firing [1][8]. Other parameters in the equations do not have specific physiological meaning.

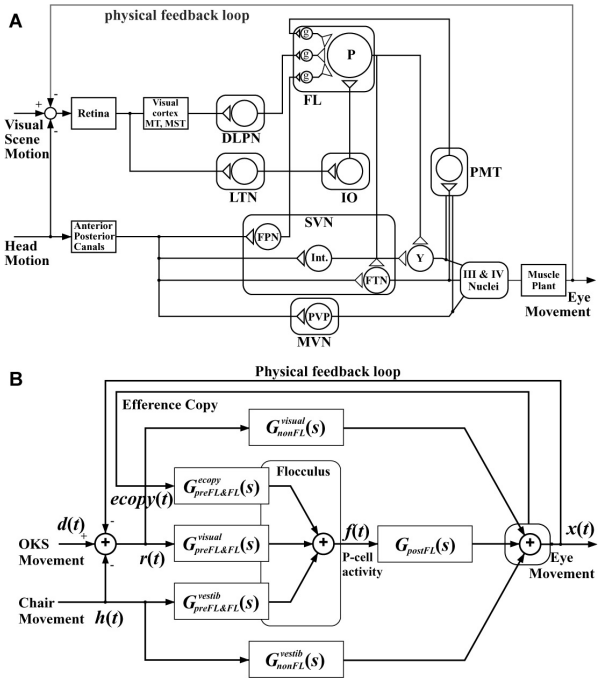

Figure 1: Vertical VOR and OKR neuronal circuit (A) and model (B). In A, FPN and FTN are the floccular (FL) projecting neurons and the FL target neurons in superior vestibular nuclei (SVN), respectively, Y is dorsal Y group, Int. is the inter-neurons in SVN projecting to Y group. P is a FL Purkinje cell and g is a granular cell. PVP is position vestibular pause neurons in medial vestibular nuclei (MVN). MT, MST and DLPN are the middle temporal visual area, the medial superior temporal area and the dorsolateral pontine nuclei, respectively. MN, extraocular motor neurons. LTN, lateral terminal nucleus of the accessory optic system. In B, $G^{ecopy}_{preFL\&FL}(s)$, $G^{vestib}_{preFL\&FL}(s)$ and $G^{visual}_{preFL\&FL}(s)$ are pre-FL/FL subsystems each of which represents a transfer function of pre-FL/FL efference copy pathway, vestibular pathway and visual pathway, respectively. The three components are added in the FL and form the Purkinje cell SS output. $G_{postFL}(s)$ represents a transfer function of post-FL pathway which transfers the Purkinje cell simple spike activity to a part of the motor command. $G^{visual}_{nonFL}(s)$ and $G^{vestib}_{nonFL}(s)$ represent transfer functions of non-FL visual and vestibular pathways, respectively. Corresponding neuronal circuit to $G^{visual}_{nonFL}(s)$ is not shown in A. $h(t)$, $d(t)$, $r(t)$, $f(t)$, $ecopy(t)$, and $x(t)$ are head position, optokinetic stimulus position, retinal slip position, FL Purkinje cell simple spike firing pattern, efference copy signal, and eye position, respectively.

Experiment

Two adult male squirrel monkeys were utilized for these experiments. For head fixation, a stainless steel bolt was secured to the occiput. This bolt fit into a receptacle on the monkey chair to fix the head. The scleral search coil method was used for eye movement recording. A stainless steel recording chamber aimed at the FL was implanted and secured to the skull. All these surgical procedures and experiments were approved by the Animal Welfare and Use Committee of Washington University.

Animals were seated in a primate chair with their heads fixed. The chair was placed in the center of a white cylindrical screen 1m in diameter (extending 36cm above and 50cm below the animal's head) on which black random dots were projected. This is the optokinetic stimulus (OKS). The right side of the animal was placed down so that rotation of the OKS about an earth vertical axis produced upward or downward nystagmus. Horizontal and vertical eye position, OKS velocity, and chair velocity were continuously digitized at a sampling frequency of 200Hz with the use of a CED 1401 interface (Cambridge Electronic Design) for display and storage using the Spike-2 program. The output of a threshold detector, signaling the occurrence of action potentials, was sampled with a resolution of 0.01 ms and stored in the same way. Raw data were also stored on VCR tape (Neurodata PCM) for the offline isolation check.

FL and ventral paraflocculer vertical zone Purkinje cells were identified by the occurrence of complex spikes and by their characteristic simple spike discharge patterns during vertical visual-vestibular interaction paradigms. Once a single unit was isolated, OKR, VOR and other visual-vestibular interaction stimuli were applied for 1 minute each. The visual-vestibular interaction paradigms used were VOR suppression (VORs) and the VOR enhancement (VORe) in which OKS moves in-phase and 180 deg out of phase with the head rotation, respectively. The maximum amplitude of head rotation and OKS were limited to 40 deg/s to assure experimentation within the linear range of the system. We used sum-of-sines (SOS)

stimuli that consisted of 5 frequencies (0.05, 0.27, 0.5, 1.27, 2.5Hz) to identify the wide band responses of the VOR/OKR system. We also applied conventional single frequency stimuli (0.1, 0.5, 2.5Hz).

Data handling

Purkinje cell firing rate was calculated from spike occurrence time by counting the number of spikes in a bin. The bin size 0.005 seconds (sampling frequency 200Hz) corresponds to the sampling interval of other data. Saccades and post-saccadic drifts if any were eliminated from the eye movements data and corresponding Purkinje cell firing rate data. After the desaccading process, firing rate data from different cells measured during the same paradigm were averaged. Anatomical plausibility of the averaging is that multiple Purkinje cells converge to a target vestibular neuron called FL target neuron (FTN). The dessacaded eye movement data measured simultaneously with those Purkinje cell firings were also averaged. These averaged data were used for parameter estimation.

Parameter estimation and verification of the model

Model parameters were determined by fitting model output to experimentally measured eye movements and FL Purkinje cell firing pattern during the VORe with SOS paradigm simultaneously. The VORe with SOS paradigm was chosen because all the subsystems in the model are activated in a wide frequency range, and the largest range of model output (eye movements) is induced during this paradigm. More than 20 samples of Purkinje cell firing rates were averaged to prepare the firing pattern for the parameter estimation. The parameter estimation was done by a nonlinear optimization method (BFGS [7]) implemented on Matlab Simulink (Mathworks).

Once a best set of parameters was estimated, the validity of the model was tested by predicting eye movements and Purkinje cell firing patterns during other paradigms at other frequencies. In addition, VOR and OKR after inactivation of the FL were simulated to compare experimental results in monkey [10] for the same purpose.

RESULTS

Parameter Estimation

Figure 2 illustrates results of the model fitting to experimental eye movement (upper panel) and Purkinje cell firing pattern (middle panel) during the VORe with the SOS paradigm (lower panel). Thick lines indicate experimental data averaged over more than 20 samples and thin lines are model output. In both upper and middle panels, eye velocity and Purkinje cell firing patterns reproduced by the model fit the experimental data well. The estimated parameters are shown in Table 1.

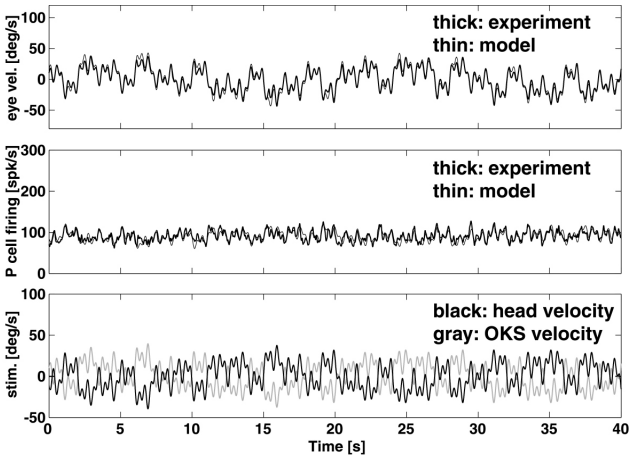

Figure 2: Results of the model fitting to experimental eye movement (upper) and Purkinje cell firing pattern (middle) during the VORe with the SOS paradigm (lower). Thick lines are experimental data and thin lines are model output.

Table 1: Model parameters estimated by the model fitting shown in figure 2.

pre-FL pathway			non-FL, post-FL pathway		
$G^{visual}_{preFL\&FL}(s)$	a_r	-1.30E-4	$G^{visual}_{nonFL}(s)$	a_r	-0.0470
	b_r	-0.0879		b_r	-0.0987
	g_r	0.0904		c_r	-0.1821
	p_r	0.122		u_r	-0.1905
				v_r	-1.696
				t_r	1.07E-6
$G^{vestib}_{preFL\&FL}(s)$	a_h	-0.125	$G^{vestib}_{nonFL}(s)$	a_h	0.0395
	b_h	-0.609		b_h	1.507
	g_h	0.162		c_h	-0.370
	p_h	0.0137		u_h	-0.0294
				v_h	-1.934
				t_h	9.06E-5
$G^{vestib}_{preFL\&FL}(s)$	a_e	-0.161	$G_{postFL}(s)$	a_x	-0.129
	b_e	-0.825		b_x	-1.044
	g_e	-0.011		c_x	9.20E-4
	p_e	0.027		t_x	4.77E-3

Verification of the model

Figure 3 illustrates results of the prediction during VORd, OKR, VORs, VORe at 0.1, 0.5, and 2.5Hz in the same format as in Figure 2 except that all samples measured in each paradigm are superimposed to show the degree of variability in the experimental data in stead of showing averaged traces and that the stimulus traces are omitted. In all the paradigms at all the frequencies examined, the model can predict experimental data well, demonstrating the generality of the model.

To further test the model validity, we simulated lesion experiments in monkeys. It has been demonstrated that flocculectomy did not change VOR gain while it reduced the OKR gain significantly. Also, the monkey's ability to make rapid modifications of the VOR such as enhancement or suppression was severely degraded [10]. In the model, flocculectomy can be simulated by disconnecting the output of FL to the post-FL subsystem.

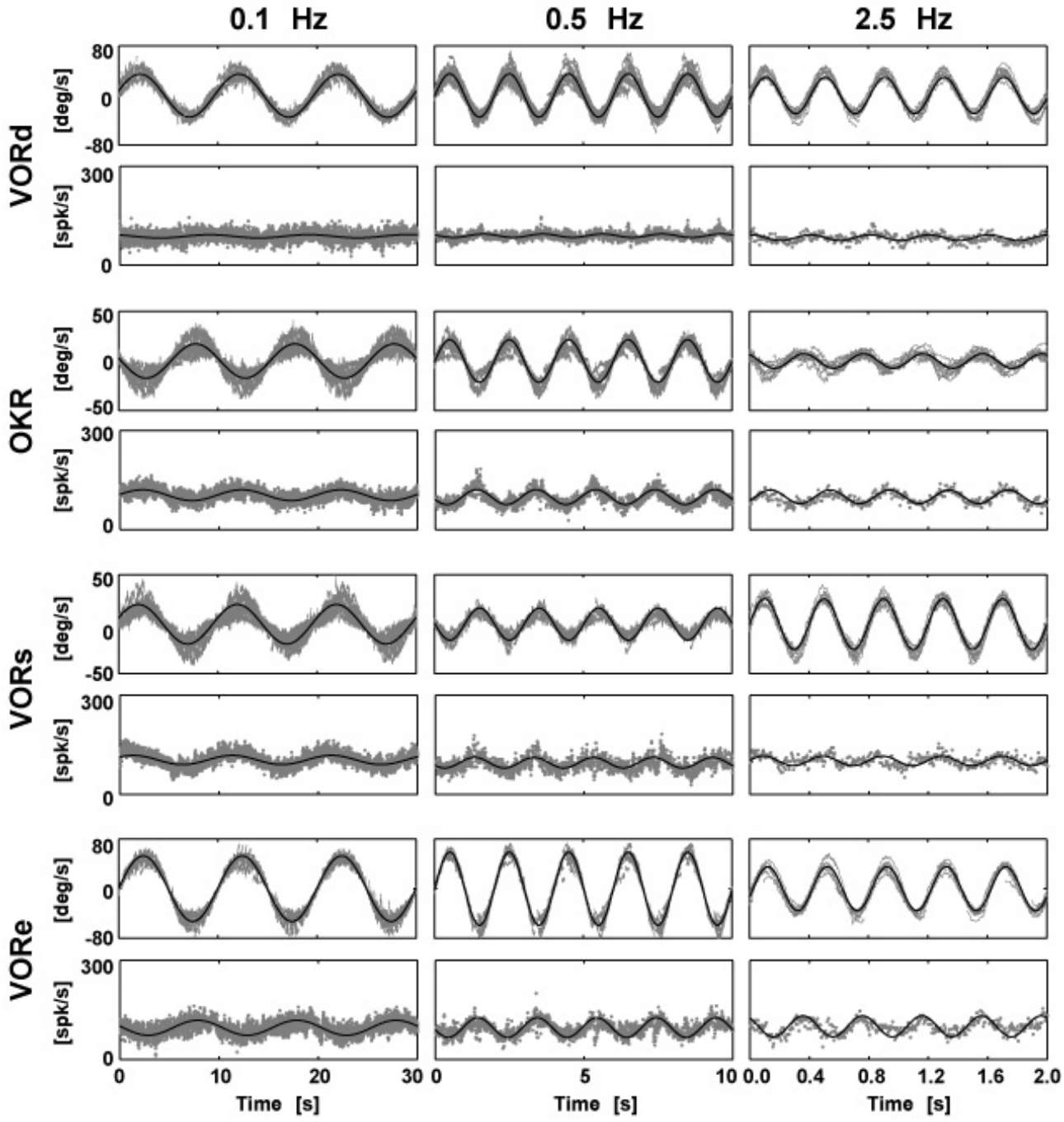

Figure 3: Results of the prediction during VORd, OKR, VORs, VORe at 0.1, 0.5, and 2.5Hz in the same format as in Figure 2 except that all the experimental data are superimposed instead of showing their average and that the stimulus traces are omitted.

Figure 4 illustrates simulated eye velocities during VORd, OKR, VORs, and VORe before (solid line) and after flocculectomy (dashed line). As demonstrated in the behavioral experiment [10], the simulation results show small change in eye velocity during VORd, significant reduction during OKR and degraded enhancement and suppression during VORe and VORs, respectively.

CONCLUSION

VOR adaptation has been an attractive model for elucidating the mechanisms of neural motor control and learning because of its well documented anatomy and easiness of observation of input and output signals. However the neuronal circuitry forms multiple feedbacks that recursively connect neural signal processing units and make it difficult to understand the signal flows and causality in the observed neuronal activity. A mathematical model whose structure reflects the anatomy is required to overcome these difficulties. There have been several models developed to simulate the VOR and its motor learning. However, only a few models [2] were quantitatively constructed based upon real experimental data and enable quantitative interpretation of their simulation results.

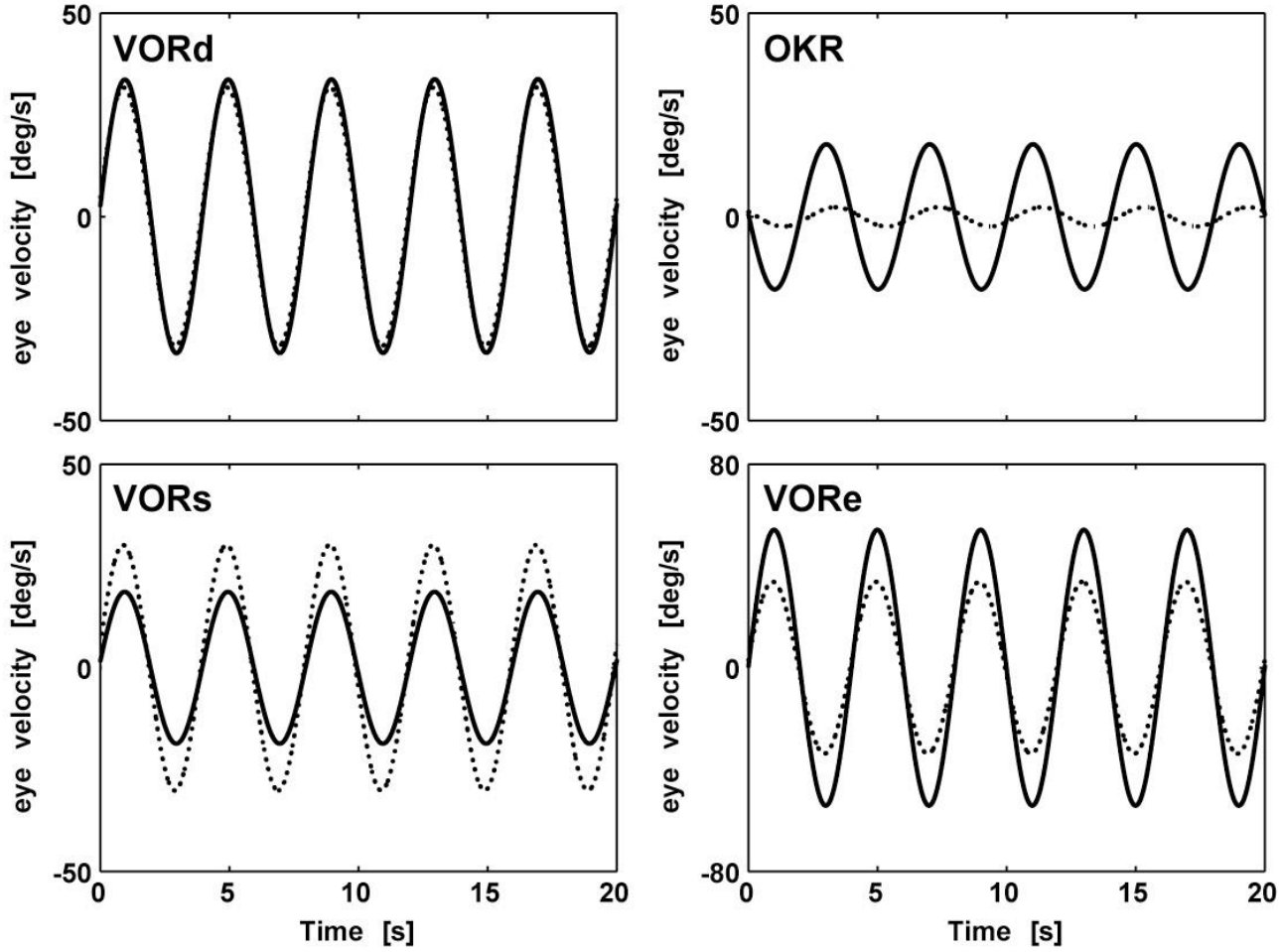

Figure 4: Simulation of the flocculectomy. Eye velocities before (solid lines) and after the flocculectomy (dashed lines) are superimposed.

The model currently constructed is quantitative and anatomically plausible. It was described around the cerebellar flocculus (FL) that has been known to play a pivotal role in the VOR motor learning, that is, pathways that include FL (FL pathway) and those that do not (non-FL pathway) were separately formulated and the former was further divided into pre- and post-FL pathways. Also, in each FL and non-FL pathway, those processing each sensory modality were explicitly described. Thus the model may provide separate information on signal processing in each pathway and its role in the VOR and its motor learning. The model parameters were determined by using experimental FL Purkinje cell firing patterns and eye movements in response to visual-vestibular mismatch stimuli that cover most of the dynamic range of the VOR/OKR system in squirrel monkeys. We demonstrated the model validity and generality by predicting FL Purkinje cell firing patterns and eye movements during other various visual-vestibular interaction paradigms and reproducing those after FL lesion.

The model is linear in that all the subsystems are described as linear systems and combined linearly. The fact that the model could quantitatively reproduce eye movements and FL Purkinje cell firing patterns during various visual-vestibular interaction paradigms indicates that the monkey vertical VOR/OKR system behaves linearly within the stimulus range currently employed. The model can be used to elucidate multimodal signal transformation in the cerebellum and to pinpoint a site or sites responsible for VOR motor learning in future studies.

Acknowledgements

We thank Drs. Pablo Blazquez, Andrea Green, Gavin Perry and Hide Tsuneoka for their valuable discussion on the model. Pat Keller provided animal care and technical support. Supported by NIH EYE grant EY-05433, a Grant-in-Aid for Scientific Research on Priority Areas(C)-Advanced Brain Science Project-from Ministry of Education, Culture, Sports, Science and Technology, Japan, and the Hori information science promotion foundation.

REFERENCES

[1] H. Gomi, M. Shidara, A. Takemura, Y. Inoue, K. Kawano, M. Kawato, Temporal Firing Patterns of Purkinje Cells in the Cerebellar Ventral Paraflocculus

during Ocular Following Responses in Monkeys I. Simple Spikes, J. Neurophysiol. 80(1998) 818-831.
[2] Y. Hirata and S.M. Highstein, Acute Adaptation of the Vestibuloocular Reflex: Signal Processing by Floccular and Ventral Parafloccular Purkinje Cells, J. Neurophysiol. 85(2001) 2267-2288.

[3] M. Ito, Cerebellar flocculus hypothesis. Nature, 363(1993) 24-25.

[4] Y. Kobayashi, K. Kawano, A. Takemura, Y. Inoue, T. Kitama, H. Gomi and M. Kawato, Temporal Firing Patterns of Purkinje Cells in the Cerebellar Ventral Paraflocculus during Ocular Following Responses in Monkeys II. Complex Spikes, J. Neurophysiol. 80(1998): 832-848.

[5] S. G. Lisberger, F. A. Miles, D. S. Zee, Signals Used to Compute Errors in Monkey Vestibulo-Ocular Reflex: Possible Role of Flocculus. J. Neurophysiol. 52(1984) 1140-1153.

[6] S. G. Lisberger and T. Sejnowski, Motor learning in a recurrent network model based on the vestibulo-ocular reflex. Nature, 360(1992) 159-161.
[7] E. Polak, Computational Methods in Optimization (Academic, New York, 1971).

[8] M. Shidara, K. Kawano, H. Gomi and M. Kawato, Inverse Dynamics Model Eye Movement Control by Purkinje Cells in the Cerebellum, Nature 365(1993) 50-52.

[9] A. Takemura, Y. Inoue, H. Gomi, M. Kawato, K. Kawano. Change in neuronal firing patterns in the process of motor command generation for the ocular following response. J. Neurophysiol. 86(2001) 1750-1763.

[10] D.S. Zee, A. Yamazaki, P.H. Butler, G. Gucer, Effects of Ablation of Floccular and parafloccular on Eye Movements in Primate. J. Neurophysiol. 46(1981) 878-899.